**ISSN 1454 - 8003**
**Proceedings of 2022 International Conference on Hydraulics and Pneumatics - HERVEX**
*November 9-10, Băile Govora, Romania*

# DYNAMICAL ASPECTS OF PNEUMATIC PROPULSION OF A PELLET

**Bogdan-Marian ȘERBAN[1,2], Andrei-Alexandru BENESCU[1,2,*], Alexandru-Polifron CHIRIȚĂ[1]**

[1] Hydraulics and Pneumatics Research Institute INOE 2000-IHP, Bucharest, Romania

[2] Mechanical Engineering, Mechatronics and Robotics Department, Politehnica University of Bucharest, Bucharest, Romania

*benescu.ihp@fluidas.ro

***Abstract:*** *In this paper, the dynamic aspects of the pneumatic propulsion of a pellet are presented. The numerical simulation was performed in the Simcenter AMESim program. Mechanical, pneumatic and signal component libraries were used; the air model used is an advanced (real) dry air model, namely the Redlich - Kwong - Soave model, in order to obtain results as close as possible to reality. The variation in time of the piston and pellet parameters with different masses, the variation of displacement versus velocity, the force exerted by the piston on the pellets and the pressure in the pneumatic chamber were determined.*

***Keywords:*** *Pneumatic propulsion, numerical simulation, dynamical aspects*

## 1. Introduction

Nowadays, the most important aspect of air use is its ability to be compressed. Thus, since pressure is defined as force divided by surface area, pressure can be converted into force, which applied to a piston in a circular bore, can produce translational displacement [1].
The disadvantages of pneumatic equipment lie in its limitations: both the forces and moments produced by pneumatic motors are low and the compressibility of the air prevents precise adjustment of operating parameters [2].
Beater presented the basic concepts of pneumatic (air) propulsion [3]. In this paper, some of the more dynamic aspects of pneumatic propulsion will be addressed, in particular the use of mechanical components and pistons.
Pneumatic pistons are cylinders that convert air pressure into mechanical force. The study of this force includes the investigation of motion, velocity and the effect of friction. There are many ways to determine the dynamics of pneumatics, but researchers most often use either a vector or a moment-balance approach[4].
Special attention is paid to the effect of the piston's weight on the pellet's dynamics. According to the simulations, the pellet's acceleration and deceleration phases are affected by the weight of the piston. It fluctuates as a function of the system's compressional and thermal properties, and it is not possible to determine the precise force exerted by the system on the pellet without a detailed analysis. However, it is possible to make some general statements about the nature of the force. The force exerted by the system on the pellet will be greater when the system is close to its equilibrium state.
A typical spring-powered air propulsion system can be seen in figure 1. The trigger sear and its connection to the trigger blade are substantially simplified in the top example, which depicts the system action in the cocked position. Trigger geometry is far more complicated than what is seen in the figure. The system's motion is seen in the bottom picture after it has fired but before the projectile has made it all the way to the barrel's muzzle [5].

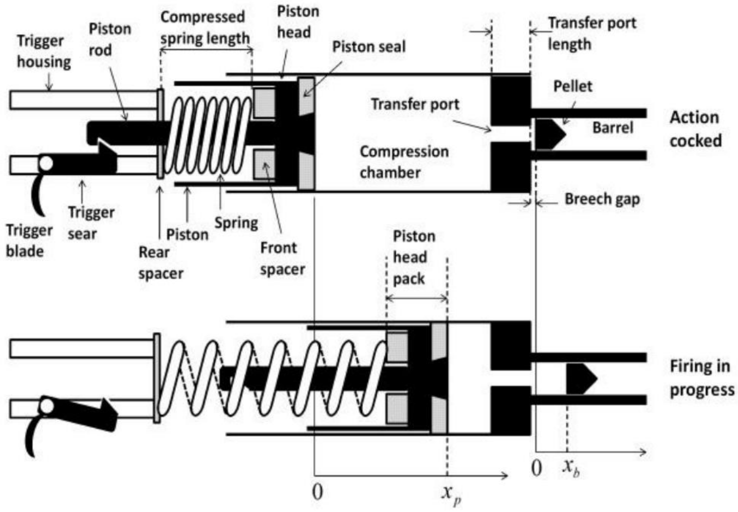


**Fig. 1.** Pellet propulsion diagram [5]

As seen in the image, a pellet is propelled forward by the compressed air resulted from the action of the spring. Frequently, the front of the spring contacts a spacer, whereas the back of the spring contacts a flat washer. The front spacer's function is to support the spring and increase the piston's total weight. Controlling the deflection energy held by the spring is the function of the rear spacer.
A transfer port is used to send high-pressure air to the breech. Through the transfer channel, the transfer port joins the breech and compression chamber.
The compression chamber will withstand some of the high-pressure air during firing, and the compression chamber model is created to include both cavities or pockets in the seal itself, where high-pressure air can become trapped when the firing mechanism is activated. The compression chamber model geometry is depicted in figure 2. It is obvious that seal cavities can be dealt with by effectively changing the chamber capacity, but the transfer channel needs further consideration [5].
If the piston's journey reaches its design-working stroke, it stops and bounces backward. For high-performance spring-piston propulsion systems, this is the most typical scenario, in which the piston physically hits the chamber end after reaching it. The pellet has not yet left the honed pipe at this point as the piston velocity reduces to zero. The piston then springs backward. As a result, the spring partially recompresses and its velocity acquires negative values [4]. This makes the piston and the spring oscillate and cause an increase in the pellet velocity.

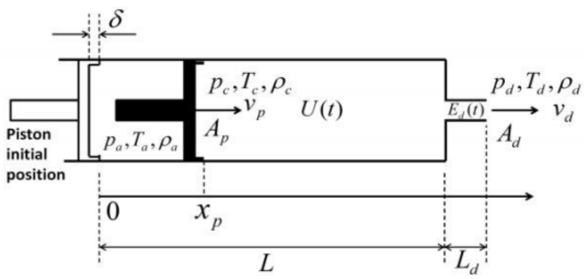


**Fig. 2.** Compression chamber diagram [5]

The thermodynamic parameters at the transfer port plane are computed beginning with the discharge pressure. Below a certain breech pressure, the flow at the transfer port turns sonic, and that value is:

$$p^*_d = p_c \left(\frac{2}{\gamma+1}\right)^{\frac{\gamma}{\gamma-1}} \tag{1}$$

Where:

$\gamma = \frac{Cp}{Cv}$

$p_c$ – the pressure of the pressure chamber
$p_d$ – pressure discharge

Figure 3 shows the design of the honed pipe and the pellet. This measurement considers the transfer port's spacing as well as the pellet's resting depth in the breech. This distance is crucial for thermodynamics and affects the numerical conditioning of the differential equations that characterize the issue.

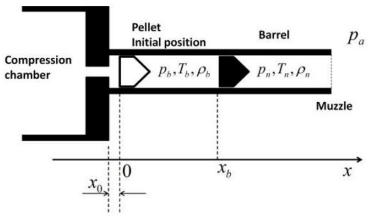


**Fig. 3.** Honed pipe diagram [5]

$$\frac{d}{dt}[(x_0 - x_b)p_b] = C_b * \eta_b * \dot{m} \tag{2}$$

Where:

$$\eta_b = \frac{A_d}{A_b}$$

$\dot{m}$ – mass flow rate

$$\frac{d\rho_b}{dt} = \frac{C_d * \eta_b * \dot{m} - v_b * \rho_b}{(x_0 + x_b)} \tag{3}$$

Where:

$v_b = \frac{dx_b}{dt}$ – the speed of the pellet

Both a direct calculation from the model and the use of influence coefficients, which indicate the partial reaction of the model owing to the unit change in specific input parameters, can be used to estimate system performance, such as muzzle velocity, kinetic energy, reload duration, etc. [6, 7, 8, 9].

## 2. Material and method

The main part of this paper presents the simulation made in AMESim environment (Fig. 4). As so, the principle of the diagram from figure 1 has been transformed into a mathematical model that can be iterated in AMESim.
To create a numerical simulation on AMESim environment, first, a deep understanding of the mechanical and pneumatic phenomenon that occurred during the propelling process is needed. The simulation sketch is illustrated in figure 4, when the trigger is released, the helical compression spring 3, which was compressed, provides a force that is delivered to piston 4 with mass 5. The air within the pressure chamber 6 (a closed system that acts as an air spring) is compressed, propelling the pellet 9 inside the honed pipe 8, imprinting it an acceleration.

An advanced dried air model has been used (Redlich - Kwong – Soave) in combination with viscous friction for the moving parts to get results as close to reality as possible. The values used for the simulation can be found in Table 1.

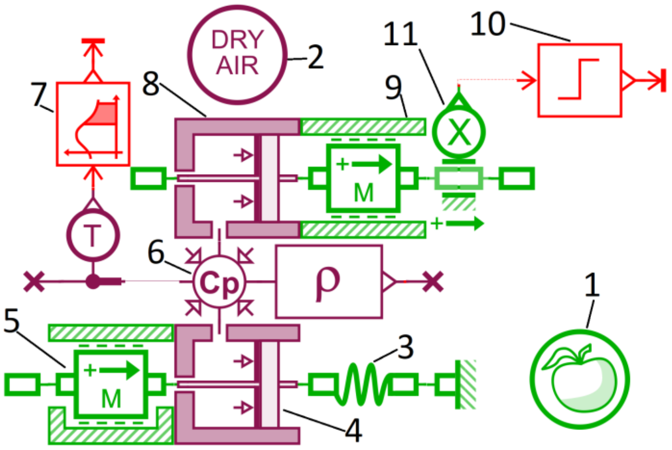


**Fig. 4.** Simulation model developed in AMESim

**Table 1:** Simulation model components

| Number | Simulation component | Value | Unit |
|---|---|---|---|
| 1 | Gravitation force | g = 9.801 | [m/s^2] |
| 2 | Dried air model | Advanced model: Redlich - Kwong - Soave | Null |
| 3 | Helical spring | spring rate = 3500 | [N/m] |
| | | spring pre-tension force = 400 | [N] |
| 4 | Pneumatic chamber | piston diameter = Ø0.02 | [m] |
| 5 | Piston mass | displacement = 0.08 | [m] |
| | | mass = 0.15 | [kg] |
| | | coefficient of viscous friction = 8 | [N/(m/s)] |
| | | restitution coefficient = 0.01 | Null |
| | | higher displacement limit = 0.08 | [m] |
| 6 | Pneumatic volume | initial temperature = 19.85 | [degree C] |
| | | volume = 1e-05 | [L] |
| 7 | Moving average | iteration period = 0.15 | [s] |
| 8 | Honed pipe | diameter = Ø0.05 | [m] |
| 9 | Pellet | **pellet mass = 0.0005 (reference value)**<br>pellet mass = 0.0008<br>pellet mass = 0.001<br>pellet mass = 0.0015 | [kg] |
| | | coefficient of viscous friction = 3 | [N/(m/s)] |
| 10 | Trigger | 0.11 | [m] |
| 11 | Displacement sensor | gain = 1 | Null |

## 3. Results of virtual experimentation

Based on the AMESim simulation network from the previous chapter and the parameters indicated in table 1, the results presented below were obtained:

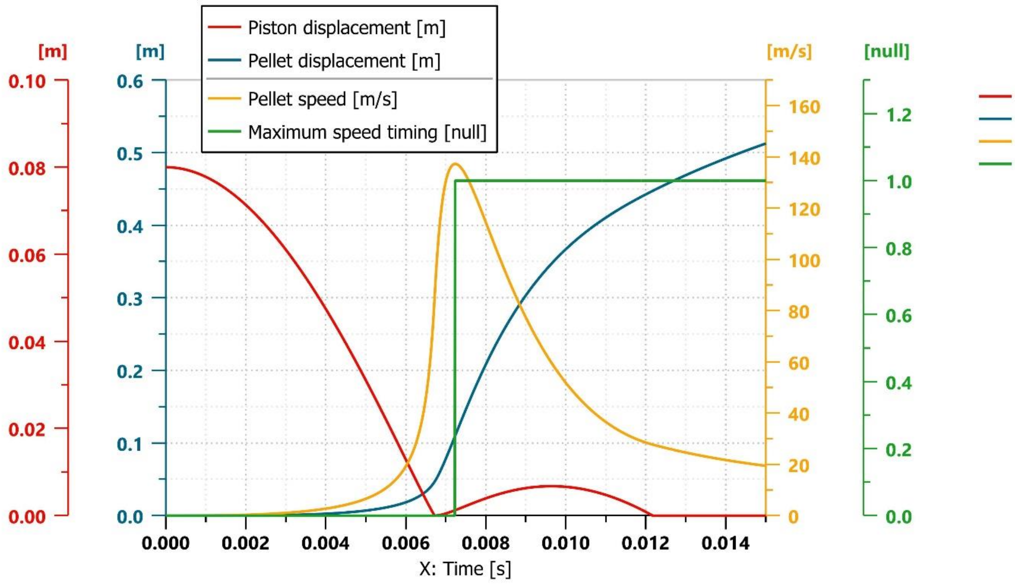


**Fig. 5.** Parameters time variation of piston and pellet

Figure 5 shows the evolution of displacement of both piston and pellet, also the speed of the pellet, which reaches its maximum value at the trigger point x = 0.00723 [s]. The graphic also highlights the restitution – movement of the piston after it reaches the higher displacement limit.

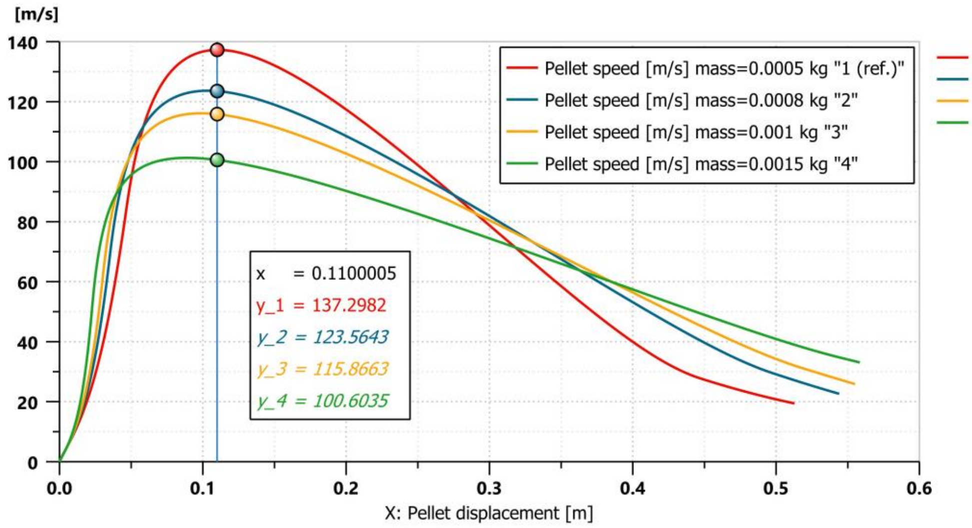


**Fig. 6.** XY Variation of displacement versus velocity

Figure 6 presents a set of simulations made to highlight the limit distance traveled by the pellet before losing speed (x = 0.11 [m]). The pellet mass also influences the maximum speed it can reach, the heavier the pellet results in a reduced threshold speed and a longer distance traveled.

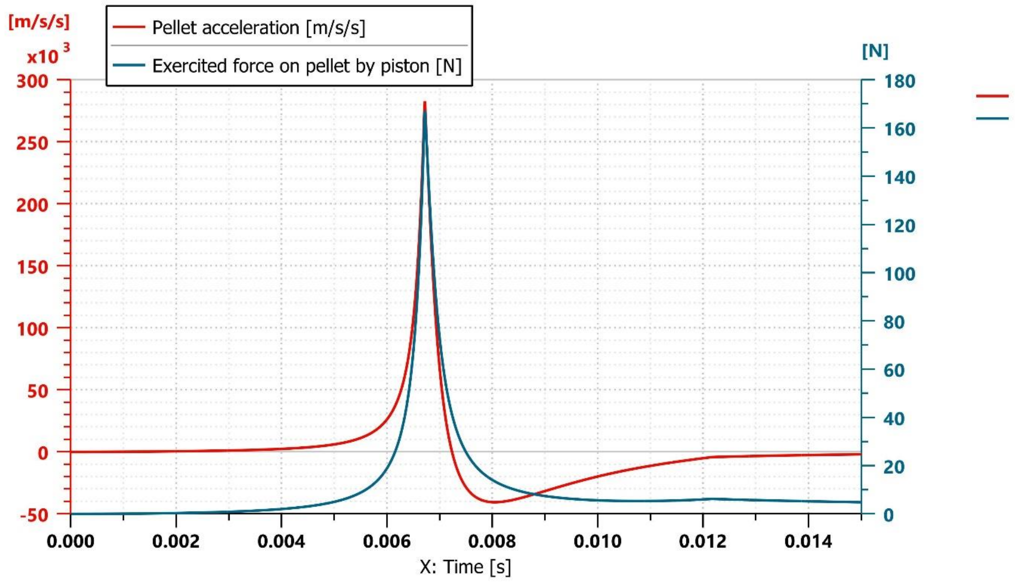


**Fig. 7.** XY Force exercised by the piston on the pellet and the pellet acceleration in time

In Fig. 7, it is shown that the pellet is accelerated by a net force imposed by the air compressed by the piston. The resistive force is proportional to the velocity of the pellet relative to the average force exerted by a piston on a pellet.

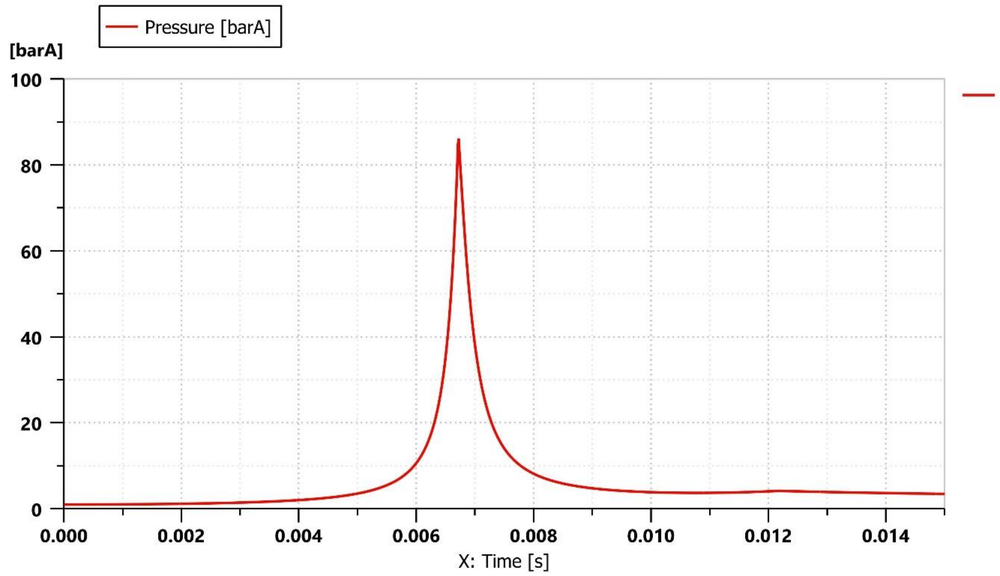


**Fig. 8.** Pressure in the pneumatic chamber

Because the pressure inside the chamber is greater than the atmospheric pressure. This pressure difference causes a decrease in air resistance and an increase in pneumatic power.
The maximum pressure that can be exerted on the pellet is determined by the ratio between the diameters of the pneumatic chambers and the honed pipe and the force generated by the helical compression spring.
After the pellet is propelled, the spring must be recompressed and the piston must be returned to its starting position (a displacement of 80 [mm]) in order to produce a repeatable occurrence. A lever

mechanism (lever ratio $^{0.25}/_{0.08}$) has been included since the amount of force required to perform this motion directly is just too great (Fr = 680 [N]).

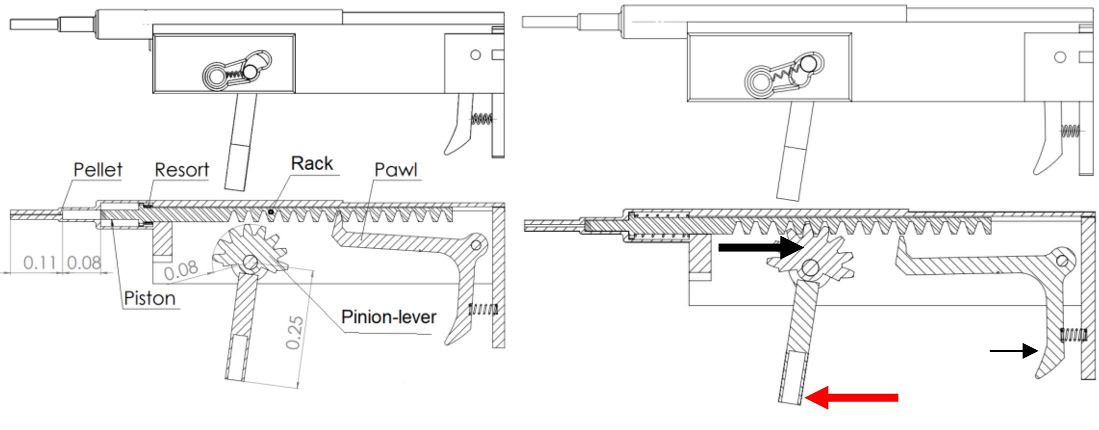


**Fig. 9.** Section diagram of the lever–piston mechanism

Figure 9 shows the three components of the lever mechanism based on the Lifting-jack patent [10]: the rack, the pawn, and the pinion-lever. To prevent the pinion from restricting the rack movement, which is prevented by the pawl in figure 9.a, the torsion spring pulls the pinion-lever to the bottom of the slot. This allows the spring to remain compressed until the trigger is pulled. The forces, velocities and displacements of the mechanism can be seen in figure 10.
Figure 9.b shows the spring decompressing, the pellet being propelled, and the trigger is pushed. The lever-pinion is thus raised in the slot and engaged with the rack to recompress the spring. The rack slides easily because of the pawl design.

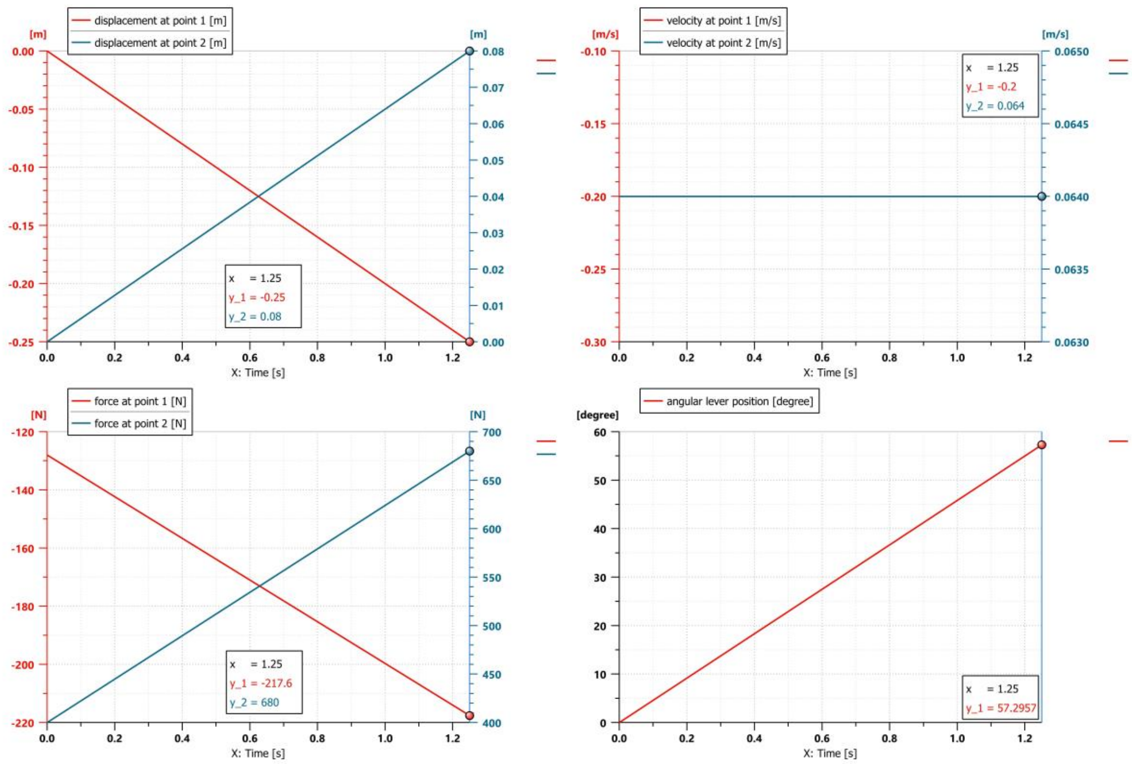


**Fig. 10.** Parameters of the lever – piston mechanism

## 4. Conclusions

In this study, the mathematical model of the spring-powered air propulsion system operation has been developed using AMESim simulation environment. Models used for the air, gravitation and friction are very complex and close to reality.

It has been demonstrated that the pellet mass influence the distance traveled by the pellet and its velocity, also the optimal length of the honed pipe until friction affects its speed.

The analysis enables us to understand how various design parameters and operating conditions influence the performance of spring-powered air propulsion systems, the simulation can be used to predict and help improve the performances of the system and may be used in an industrial design environment for optimization purposes.

### Acknowledgments

This paper has been financed under a project funded by the Ministry of Research, Innovation and Digitalization through Programme 1- Development of the national research & development system, Sub-programme 1.2 - Institutional performance - Projects financing the R&D&I excellence, Financial Agreement no. 18PFE/30.12.2021. European funding has also been granted, under Competitiveness Operational Programme POC 2014-2020, call POC-A1-A.1.1.3-H-2016, Financial agreement no. 253/02.06.2020, signed between INOE 2000 and the Ministry of Education and Research for the project titled “Horizon 2020 Support Center for European project management and European promotion PREPARE”, MYSMIS2014 code 107874.

### References

[1] Șerban, Bogdan. *Proportional pneumatic pressure regulator / Regulator de presiune pneumatic proportional*. Bachelor thesis. Politehnica University of Bucharest, 2022.
[2] Ryszard, Dindorf, Jakub Takosoglu, and Piotr Wos. *Development of pneumatic control systems.* Kielce, Publishing House of Kielce University of Technology, 2018.
[3] Beater, Peter. *Pneumatic Drives: System Design, Modelling and Control*. Springer Science & Business Media Publishing, 2007.
[4] Duc, Linh Do, Vladimir Horak, Roman Vítek, and Vladimir Kulish. “The internal ballistics of airguns Paper presented at the 2017 International Conference on Military Technologies (ICMT), Brno, Czech Republic, May 31- June 2, 2017.
[5] Tavella, Domingo. “Internal Ballistics of Spring Piston Airguns.” (April 2015). Available on ResearchGate, at https://www.researchgate.net/publication/274638905_Internal_Ballistics_of_Spring_Piston_Airguns.
[6] Horák, V., L. D. Duc, R. Vítek, S. Beer, and Q. H. Mai. “Prediction of the Air Gun Performance.” *Advances in Military Technology* 9, no. 1 (2014): 31–44.
[7] Plíhal, B., S. Beer, J. Komenda, L. Jedlička, and B. Kuda. *Ballistics*. Brno, Military Academy in Brno, 2003.
[8] Arsenjev, S.L., I.B. Lozovitski, and Y.P. Sirik. “The Flowing System Gasdynamics. Part 3: Saint-Venant – Wantzel’s formula modern form.” *arXiv: Fluid Dynamics* (February 2003): arXiv:physics/0302038.
[9] Johnston, I. A., and L. V. Krishnamoorthy. *A Numerical Simulation of Gas Gun Performance*. [Report DSTO-TN-0804]. Edinburgh, Defence Science and Technology Organisation, February 2008.
[10] Fraley, Robert M. *Lifting-jack*. US patent 964905A, 1909. https://patents.google.com/patent/US964905A/en?oq=US+patent+964905.